

Synthesis and characterisation of [(triphos)Fe(CO)H₂] and its protonation to a dihydrogen complex *via* an unconventional hydrogen-bonded intermediate^{†‡}

Gemma Guilera,^a G. Sean McGrady,^{*b} Jonathan W. Steed,^{*c}
Richard P. L. Burchell,^b Peter Sirsch^b and Anthony J. Deeming^d

Received (in Montpellier, France) 29th January 2008, Accepted 9th April 2008

First published as an Advance Article on the web 15th May 2008

DOI: 10.1039/b801652f

The complex [(triphos)Fe(CO)H₂] **1** has been prepared and characterised by ¹H and ³¹P NMR and IR spectroscopies, and by single-crystal X-ray diffraction. Complex **1** is fluxional at ambient temperatures in solution; NMR spectral simulation shows that both a Bailar twist of the triphos ligand and pairwise hydride exchange contribute to this fluxionality, with the latter process apparently more facile. DFT-calculated vibrational frequencies for **1** indicate that both these processes are thermally accessible at ambient temperatures. The X-ray crystal structure of complex **1** shows that the triphos ligand adopts a *fac* arrangement in a distorted octahedral structure, with the two hydride ligands mutually *cis*, and a non-linear Fe–C–O moiety. Protonation of complex **1** with hexafluoroisopropanol (HFIP) initially produces a hydrogen-bonded intermediate; reaction proceeds further to give the cationic complex [(triphos)Fe(CO)H(η²-H₂)]⁺ **2**. Complex **2** decomposes above 250 K in solution, but has been characterised by NMR spectroscopy. *T*_{1 min} and *J*_{HD} measurements indicate that **2** contains a stretched dihydrogen ligand, with *r*_{HH} = 1.03 Å, in apparent disagreement with DFT calculations that suggest that the equilibrium H–H distance is 0.85 Å, indicative of a conventional dihydrogen moiety. However, the very shallow nature of the potential energy surface for the Ru(η²-H₂) moiety can account for this difference between experimental and calculated values. The experimental and computed structural and spectroscopic features deduced for **1** and **2** are compared with those of their known ruthenium analogues, and are discussed in the context of other hydride and dihydrogen complexes of the Group 8 metals.

Introduction

With the first report by Hieber of [H₂Fe(CO)₄] in 1931,¹ carbonyl hydrides are amongst the longest known of organo-transition-metal complexes, and predate the birth of organometallic chemistry as a discipline by at least two decades. Carbonyl hydride phosphine complexes in particular have represented an area of intense research, due in part to their structural and spectroscopic diversity, but also on account of the crucial role they play—or are suspected to

play—in many metal-catalysed reactions involving CO and H₂. These include such important industrial processes as the water gas shift reaction, Fischer Tropsch catalysis, hydroformylation, reductive carbonylation and hydrogenation of alkenes.² The involvement in many of these processes of molecular hydrogen complexes is becoming increasingly widely realised.³ Furthermore, complexes of the type [L₄MH₂] and their protonation products [L₄MH₃]⁺ have played a seminal role in studies of stereochemical non-rigidity and in the understanding of molecular hydrogen complexes.⁴ We report here the synthesis and characterisation of the novel [L₄MH₂] complex [(triphos)Fe(CO)H₂] **1** [triphos = MeC(CH₂CH₂PPh₂)₃], and a study by NMR spectroscopy of its protonation *via* an intermediate proton-hydride hydrogen-bonded complex to give the cationic dihydrogen-hydride [L₄MH₃]⁺ product [(triphos)Fe(CO)H(η²-H₂)] **2**.

Results and discussion

Synthesis and characterisation of [(triphos)Fe(CO)H₂] **1**

During a study of the hydride-borohydride complex [(triphos)Fe(H)(η²-BH₄)] and its conversion to the remarkable species [(triphos)Fe(μ,η⁴:η⁴-BH₆)Fe(triphos)]⁺,⁵ we observed the formation of a small amount of a yellow by-product,

^a Experiments Division, CELLS-ALBA, Ed. C3, Campus UAB, Bellaterra, Spain

^b Department of Chemistry, University of New Brunswick, 30 Dineen Drive, Fredericton, N.B. 3B 6E2, Canada

^c Department of Chemistry, University of Durham, South Road, Durham, UK DH1 3LE

^d Department of Chemistry, University College London, 20 Gordon Street, London, UK WC1H 0AJ

[†] Dedicated to the memory of Dr D. A. 'Fred' Armitage (King's College London 1941–2008).

[‡] Electronic supplementary information (ESI) available: NMR simulations for exchange processes **A** and **B** (Scheme 1) alone; Arrhenius and Eyring plots for combined exchange involving **A** and **B**; DFT calculated structures for [(triphos')Fe(CO)H₂] **1'** and [(triphos')Fe(CO)H(η²-H₂)]⁺ **2'**. CCDC reference number 244046. For ESI or crystallographic data in CIF or other electronic format see DOI: 10.1039/b801652f

which was characterised as [(triphos)Fe(CO)H₂] **1**. Subsequent deliberate synthesis of this air-stable complex proceeded by two different routes. In the first, [Fe(H₂O)₆](BF₄)₂ was reacted with triphos and an excess of NaBH₄ in THF solution through which a stream of CO was passed. The second method drew on the procedure employed by Bakhmutov *et al.* in their synthesis of the ruthenium analogue of **1**.⁶ In this preparation, [(triphos)FeH(η²-BH₄)] was reacted with a slight excess of KO^tBu in anhydrous THF, followed by passage of CO through the solution. The IR spectrum of a solid film of **1** showed a strong band at 1880 cm⁻¹ (ν_{CO}), and a broad feature at 1663 cm⁻¹, assigned to both symmetric and antisymmetric ν_{Fe-H} modes, which could not be resolved. These features correspond to DFT-calculated harmonic frequencies of 1930 and 1921 cm⁻¹. The calculated ν_{CO} mode occurs at 2020 cm⁻¹, exhibiting strong coupling with the symmetric ν_{Fe-H} feature. The scaling factors of 0.93 and 0.86, respectively, for the ν_{CO} and ν_{Fe-H} modes reflects a greater degree of anharmonicity in the FeH₂ moiety. The ¹H NMR spectrum of **1** in CD₂Cl₂ at 298 K revealed a well-resolved pseudo-quartet in the hydride region at -10.5 ppm (*J*_{P,H} = 21 Hz). The ³¹P{¹H} NMR spectrum displayed a broad peak at 57.1 ppm. The structure of **1** determined by single-crystal X-ray diffraction (Fig. 1) shows a distorted octahedral environment around the Fe centre on account of the *fac*-symmetry imposed by the triphos ligand. The two hydride ligands are mutually *cis*, and the Fe–C–O moiety deviates from linearity by 6°. The three Fe–P distances are very similar (Fe–P_{av} = 2.196 Å), reflecting the comparable *trans* influences exerted by the hydride and carbonyl

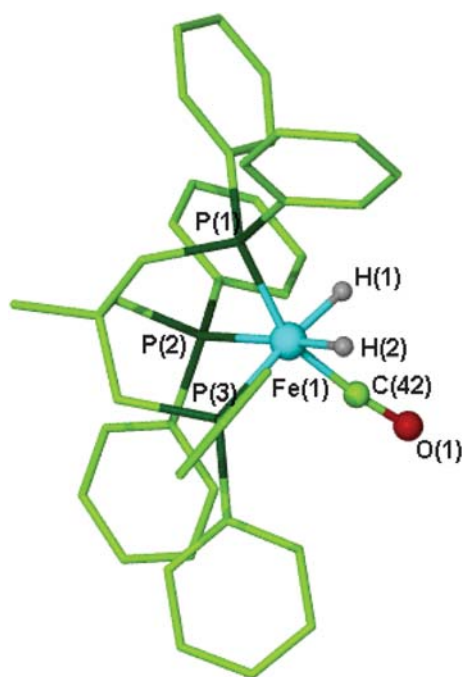


Fig. 1 X-Ray crystal structure of [(triphos)Fe(CO)H₂] **1**. Selected bond lengths (in Å): Fe–H(1) 1.57(3), Fe–H(2) 1.53(4). Fe–P(1) 2.1925(12), Fe–P(2) 2.1998(12), Fe–P(3) 2.1954(11). Selected angles (in °): H(1)–Fe–H(2) 88.7(18), C(42)–Fe–H(1) 65.6(12), C(42)–Fe–H(2) 80.6(14), Fe–C(42)–O(1) 174.0(4), P(3)–Fe–H(1) 171.0(12), P(2)–Fe–H(2) 175.6(14), P(3)–Fe–C(42) 106.69(15).

ligands. The Fe–H(1) distance is 1.57(3) Å, and Fe–H(2) is 1.53(4) Å. The molecular structure of **1** in the crystalline state is slightly less distorted than its ruthenium analogue [(triphos)-Ru(CO)H₂] **3**, reported by Bakhmutov *et al.*,⁶ although the Fe–C–O moiety in **1** deviates slightly more (2°) from linearity.

In contrast to its Ru analogue **3**, [(triphos)Fe(CO)H₂] **1** displays a non-rigid structure as revealed by ¹H and ³¹P{¹H} variable-temperature (VT) NMR spectroscopic experiments over the range 186–300 K. The pseudo-quartet observed in the hydride region of the ¹H NMR spectrum at room temperature transforms into a second-order feature at 260 K. In addition, inequivalent phosphorus nuclei are evident in the VT ³¹P{¹H} NMR spectrum, where the room temperature singlet at δ = 57.1 ppm evolves at 280 K into a triplet at δ = 61.3 ppm and a doublet at δ = 54.9 ppm (*J*_{P,P} = 39.4 Hz). ¹H NMR spectroscopy showed **1** to have a *T*_{1 min} of 208.0 ms at 210 K, in the regime expected for a classical transition-metal hydride.⁷

Fig. 2a shows VT ¹H NMR spectra of **1** in CD₂Cl₂, revealing the transformation of a quartet at 295 K (apparently equal coupling of the three ³¹P nuclei to the two ¹H nuclei) into a second-order pattern on cooling to 200 K. Simulation of these spectra (Fig. 2b) using the program gNMR reveals that the two processes described in Scheme 1 are responsible for the transformations observed. A combination of a Bailar twist (turnstile rotation)⁸ of the triphos ligand with respect to the FeH₂(CO) moiety (process **A**), together with a pairwise exchange of the hydride ligands (process **B**), accurately matches the observed spectra between 280 and 230 K.

It is clear from the simulations that pairwise hydride exchange (process **B**) is the lower energy pathway. Arrhenius and Eyring plots (see ESI†) provide the following estimates for this process: *E*_a = 24.3(4.2) kJ mol⁻¹; Δ*H*[‡] = 22.1(4.0) kJ mol⁻¹ and Δ*S*[‡] = -83.5(3.3) J K⁻¹ mol⁻¹. Presumably this exchange is facilitated by the existence of a low-lying dihydrogen complex of the form [(triphos)Fe(η²-H₂)(CO)], as is the case for a wide range of polyhydride complexes.⁹ For example, *ab initio* calculations have shown the [L₄MH₂] model systems [(CO)₄FeH₂] and [(PH₃)₄RuH₂] to undergo polytopal rearrangement

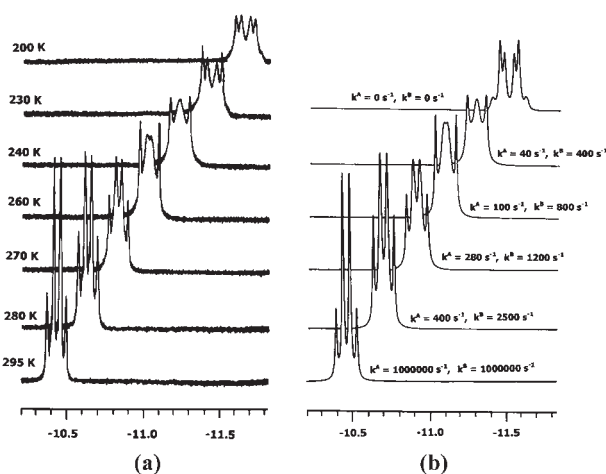
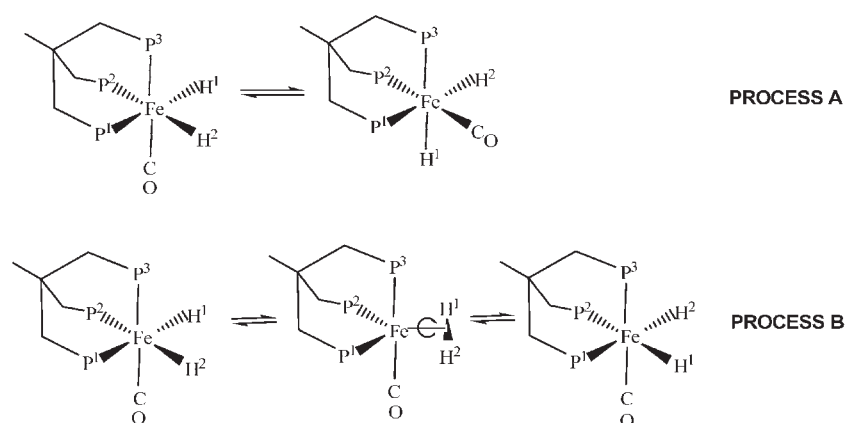


Fig. 2 VT ¹H NMR spectrum and simulation of [(triphos)Fe(CO)H₂] **1** in CD₂Cl₂, showing the loss of fluxionality and second-order behaviour below 260 K. (a) Observed spectrum; (b) simulated spectrum.



Scheme 1 Intramolecular exchange processes (Bailar twist **A** and pairwise hydride exchange **B**) used to model the VT ^1H NMR spectra of **1**.

via a square-pyramidal dihydrogen complex in which the H_2 ligand occupies an axial site.¹⁰ Although the ligand environment in **1** is more severely restrictive than in these simple model systems, the mutually *cis* hydride ligands can easily attain a similar transition-state geometry if the triphos ligand occupies two equatorial and one axial site. It is noteworthy in this regard that the more rigid complex $[(\text{tetraphos})\text{FeH}_2]$ [tetraphos = $\text{P}(\text{CH}_2\text{CH}_2\text{PPh}_2)_3$] shows fluxional behaviour in its ^1H NMR spectrum as low as 183 K.¹¹ However, compounds of the formula $[(\text{tetraphos})\text{MH}_2]^+$ ($\text{M} = \text{Co}, \text{Rh}, \text{Ir}$) have been shown to be classical dihydrides by T_1 measurements, with $\text{M}-\text{H}$ relaxation process being the major relaxation component rather than the $\text{H}-\text{H}$ relaxation process.¹² The second-row congener of **1**, *viz.* $[(\text{triphos})\text{Ru}(\text{CO})\text{H}_2]$ **3** is stereochemically rigid in solution at ambient temperatures.⁶ The stronger $\text{M}-\text{H}$ bonds generally found in second-row metal complexes are likely to stabilise the ground state dihydride in this system with respect to the putative dihydrogen transition state required for site exchange.¹³

We carried out DFT calculations on complex **1** to corroborate the experimental X-ray crystal structure (Fig. 1), and to provide further insight into the fluxionality of the complex (Scheme 1), as suggested by simulated NMR spectra (Fig. 2). In our initial calculations the six C_6H_5 substituents bound to the three P atoms of the triphos ligand were replaced with H atoms (H'). Subsequently, we were able to optimize the geometry of the full complex $[(\text{triphos})\text{Fe}(\text{CO})\text{H}_2]$ (**1**). The calculated structures of **1** and H' show good agreement with the experimentally determined structure (Fig. 3 and Fig. S1†).

Our NMR spectral simulations revealed the fluxionality of **1** to be a combination of processes **A** and **B** in Scheme 1. From the DFT-optimised geometry of **1**, normal modes of vibration that displace the geometry towards the reaction coordinate corresponding to a Bailar twist (process **A**) appear at 404 and 474 (FeH_2 deformation), and at 504 and 514 cm^{-1} (FeL_3 twist). Those corresponding to pairwise hydride exchange (process **B**) appear at 594 (coupled FeH_2/CO stretching motion), 726 (MH_2 rocking) and 826 cm^{-1} (MH_2 symmetric wag). The relatively soft vibrational characterising each of these two processes thus indicates that they are both sufficiently thermally accessible to allow the fluxional behaviour observed in solution at ambient temperatures.

Characterisation of the dihydrogen complex $[(\text{triphos})\text{Fe}(\text{CO})\text{H}(\eta^2-\text{H}_2)]^+$ **2**

First-row transition metals have a greater proclivity to produce dihydrogen complexes than do their second- and third-row congeners owing to the less diffuse nature of the 3d orbitals compared to 4d and 5d.¹³ As $[(\text{triphos})\text{Ru}(\text{CO})\text{H}(\eta^2-\text{H}_2)]^+$ **4** was already known, we prepared the analogous Fe complex $[(\text{triphos})\text{Fe}(\text{CO})\text{H}(\eta^2-\text{H}_2)]^+$ **2** by addition at low temperature of an excess (16 eq.) of the medium strength acid hexafluoroisopropanol (HFIP), $(\text{CF}_3)_2\text{CHOH}$, to a CD_2Cl_2 solution of $[(\text{triphos})\text{Fe}(\text{CO})\text{H}_2]$ **1** in an NMR tube. The ^1H NMR spectrum of the resulting complex at

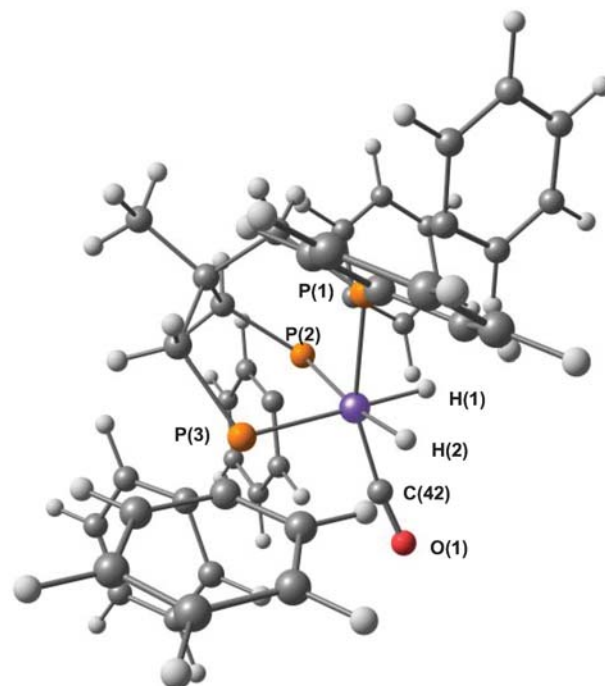
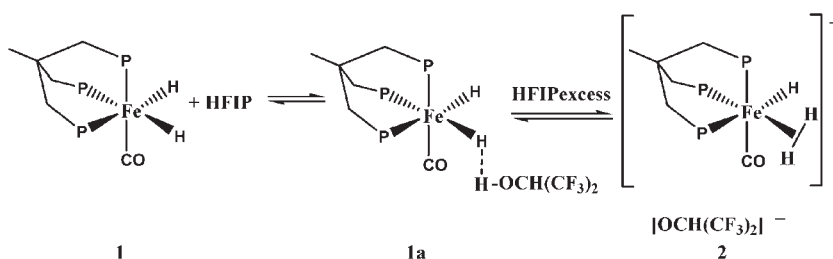


Fig. 3 DFT calculated structure of $[(\text{triphos})\text{Fe}(\text{CO})\text{H}_2]$ (**1**) calculated at the B3LYP level of theory with a 6-31G(d,p) basis set. Selected bond lengths (in Å): $\text{Fe}-\text{H}(1)$ 1.52, $\text{Fe}-\text{H}(2)$ 1.52, $\text{Fe}-\text{P}(1)$ 2.228, $\text{Fe}-\text{P}(2)$ 2.224, $\text{Fe}-\text{P}(3)$ 2.217. Selected angles (in $^\circ$): $\text{H}(1)-\text{Fe}-\text{H}(2)$ 84.5, $\text{C}(42)-\text{Fe}-\text{H}(1)$ 79.5, $\text{C}(42)-\text{Fe}-\text{H}(2)$ 78.8, $\text{Fe}-\text{C}(42)-\text{O}(1)$ 172.9, $\text{P}(3)-\text{Fe}-\text{H}(1)$ 178.1, $\text{P}(2)-\text{Fe}-\text{H}(2)$ 171.4, $\text{P}(1)-\text{Fe}-\text{C}(42)$ 157.9.



Scheme 2 Reaction pathway for the conversion of [(triphos)Fe(CO)H₂] **1** into [(triphos)Fe(CO)H(η²-H₂)]⁺ **2**.

190 K displayed a new broad hydride resonance at -8.6 ppm (3H). The short $T_{1\text{min}}$ value corresponding to this feature (20.6 ms at 210 K) argues persuasively in favour of a non-classical dihydrogen moiety. The yellow, air-sensitive complex [(triphos)Fe(CO)(η²-H₂)H]⁺ **2** is highly fluxional in solution, with fast hydride–dihydrogen exchange occurring down to 180 K. Complex **2** is stable below 250 K, but slowly eliminates H₂ above this temperature, as evidenced by the growth of a feature at $\delta = 4.6$ ppm in the ¹H NMR spectrum assigned to free H₂. In the ³¹P{¹H} NMR spectrum at 190 K, the transformation of **1** [$P_a = 61.3$ ppm (t), $P_b = 54.9$ ppm (d)] into **2** [$P_a = 41.3$ ppm (t), $P_b = 46.0$ ppm (d)] is clearly observed, as shown in Fig. 4. The phosphorus nucleus *trans* to CO is characterised by a significant low-frequency shift ($\Delta\delta = 20.1$ ppm). The conversion of **1** to **2** apparently occurs *via* the intermediate hydrogen-bonded adduct [(triphos)(CO)(H)Fe–H···H–OCH(CF₃)₂] **1a**, as depicted in Scheme 2. This conclusion is based on the observance of a low frequency temperature-dependent shift of the hydride resonance (-10.48 to -10.57 ppm at 250 K and to -10.80 ppm at 190 K) upon addition of HFIP. The results we observed are consistent with those of Shubina *et al.* in their study of the analogous complex [(triphos)Ru(CO)H₂] under protonation.¹⁴

A simple method for calculating the H–H distance in a dihydrogen complex involves partial deuteration, and relies on an inverse correlation between r_{HH} and J_{HD} for the (η²-HD) ligand, which was first proposed by Morris *et al.*¹⁵ and improved by Heinekey and co-workers.¹⁶ For [(triphos)Fe(CO)H(η²-HD)]⁺ **2-d₁** (produced by addition of CF₃CO₂D

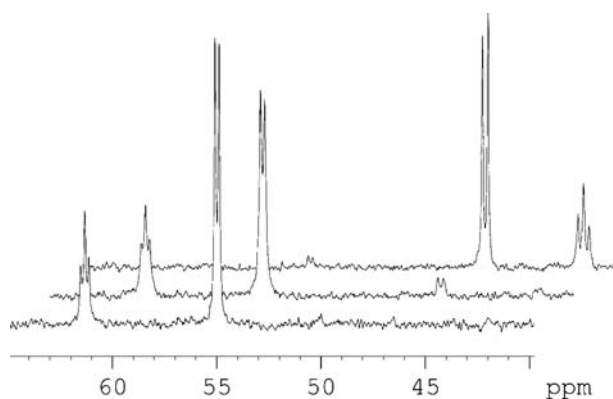


Fig. 4 ³¹P{¹H} NMR spectra in CD₂Cl₂ showing the transformation of [(triphos)Fe(CO)H₂] **1** (lower spectrum) into [(triphos)Fe(CO)(η²-H₂)H]⁺ **2** (upper spectrum) *via* the hydrogen-bonded intermediate [(triphos)(CO)(H)Fe–H···H–OCH(CF₃)₂] **1a** (middle spectrum) upon addition of (HFIP).

to **1**) a signal was observed at $\delta = -8.57$ ppm, while a second feature in the spectrum, at $\delta = -8.46$ ppm is assigned to [(triphos)Fe(CO)D(η²-HD)]⁺ **2-d₂**. Along with the characteristic resonance of free HD at $\delta = 4.60$ ppm ($J_{\text{HD}} = 43.2$ Hz), these features attest to the lability of the dihydrogen ligand in complex **2**; a modest low-frequency shift of the resonance is characteristic of a dihydrogen complex.^{17–19} Unfortunately these resonances are broad and we were unable to determine the value of J_{HD} reliably. The $T_{1\text{min}}$ method proposed by Hamilton and Crabtree affords a more precise estimate of the H–H distance,^{20a} and this approach was employed in a study of the Ru analogue **4**, the H–H distance in which was accurately estimated using the $T_{1\text{min}}$ slow-spinning model.⁶ Accordingly, we carried out a similar analysis of complex **2**. Insertion of our experimental values ($T_{1\text{min}}$ for **1** = 208.06 ms and $T_{1\text{min}}^{\text{obs}}$ for **2** = 20.61 ms) into eqn (1) (which accounts for the averaging of $T_{1\text{min}}$ by the exchange process) gives $T_{1\text{min}}^{\text{obs}}$ ($2_{\text{Fe}(\text{H}_2)}$) = 14.21 ms, and substitution of this value into eqn (2) to obtain the true dipole–dipole relation time gives $T_{1\text{min}}$ ($2_{\text{Fe}(\text{H}_2)}$) = 15.25 ms. The H–H distance of the dihydrogen ligand in **2** can now be obtained from eqn (3). According to the fast- ($C^* = 0.7937$) and slow-rotation ($C^* = 1$) models, the empirical r_{HH} values for complex **2** are 0.816 and 1.03 Å, respectively. The small relaxation due to phosphorus was neglected in order to make the analysis exactly comparable with the Ru analogue.^{20b} As analogous dihydrogen complexes containing different metal centres present the same spinning behaviour,²¹ and as the fast-rotation model can be ruled out for the Ru analogue, we are confident that slow rotation also applies to **2**, giving r_{HH} (**2**) = 1.03 Å. The NMR results thus imply that [(triphos)Fe(CO)H(η²-H₂)] **2** contains a slightly stretched dihydrogen ligand, in contrast to the Ru analogue **4** ($r_{\text{HH}} = 0.92$ Å by J_{HD} and 0.94 Å measured by $T_{1\text{min}}$), which contains a normal dihydrogen moiety.

$$1/T_{1\text{min}}^{\text{obs}}(2_{\text{Fe},\text{H}_3}) = (1/3)/T_{1\text{min}}(1_{\text{Fe},\text{H}_2}) + (2/3)/T_{1\text{min}}^{\text{obs}}(2_{\text{Fe}(\text{H}_2)}) \quad (1)$$

$$1/T_{1\text{min}}^{\text{obs}}(2_{\text{Fe}(\text{H}_2)}) = 1/T_{1\text{min}}(1_{\text{Fe},\text{H}_2}) + 1/T_{1\text{min}}(2_{\text{Fe}(\text{H}_2)}) \quad (2)$$

$$r_{\text{HH}} [\text{Å}] = 5.815 C^* (T_{1\text{min}}/\nu)^{1/6} \quad (3)$$

$T_{1\text{min}}(1_{\text{Fe},\text{H}_2})$ = minimum spin–lattice relaxation time of the hydride nuclei in complex **1**.

$T_{1\text{min}}^{\text{obs}}(2_{\text{Fe},\text{H}_3})$ = observed minimum spin–lattice relaxation time of the hydride resonance in complex **2**.

$T_{1\text{min}}^{\text{obs}}(2_{\text{Fe}(\text{H}_2)})$ = observed minimum spin–lattice relaxation time of the dihydrogen ligand in complex **2**, calculated from eqn (1).

$T_{1 \text{ min}}(\mathbf{2}_{\text{Fe}(\text{H}_2)}) =$ minimum spin–lattice relaxation time of the dihydrogen ligand in complex **2**, calculated from eqn (2).

This conclusion runs counter to the expected change in behaviour on going from a first-row transition-metal complex to its second-row analogue. The strength of $\text{M} \rightarrow (\eta^2\text{-H}_2)$ back-bonding largely determines whether $[\text{L}_n\text{MH}_2]$ or $[\text{L}_n\text{M}(\eta^2\text{-H}_2)]$ is formed.²² The general trend down a transition-metal triad is an increase in M-H bond strength and a corresponding stabilisation of the dihydride oxidative addition product as the metal changes from 3d through 4d to 5d.²³ For example, Group 9 complexes of the type $[(\text{tetraphos})\text{MH}_2]^+$ are reported to be non-classical in the solid state and solution only when $\text{M} = \text{Co}$; the Rh analogue is possibly non-classical in solution whereas the Ir version is classical in both phases.²⁴ However, Group 8 complexes of the form $[\text{L}_4\text{MH}(\eta^2\text{-H}_2)]^+$ appear to buck this trend. In an extensive study of $[\text{trans}(\text{P}_2)_2\text{MH}(\eta^2\text{-H}_2)]^+$ complexes [$\text{P}_2 = \text{Et}_2\text{PCH}_2\text{CH}_2\text{PEt}_2$ (depe) or $\text{Ph}_2\text{PCH}_2\text{CH}_2\text{PPh}_2$ (dppe)], Bautista *et al.* concluded that the Ru dihydrogen complex is *less* stable than its Fe counterpart.²⁵ In this series of complexes, ν_{MH} modes revealed the σ -bond strength of the M-H moiety to increase in the order $\text{Fe} < \text{Ru} < \text{Os}$ as expected, whereas the $\text{M}-(\eta^2\text{-H}_2)$ bond strength was found to increase in the order $\text{Ru} < \text{Fe} < \text{Os}$; this was accompanied by a corresponding decrease in the H-H bonding interaction in the order $\text{Os} < \text{Fe} < \text{Ru}$. Hence, Fe acts as a better-than-expected $d_\pi(\text{M}) \rightarrow \sigma^*(\eta^2\text{-H}_2)$ back-donor.²⁵ In a similar vein, experimental and theoretical studies of the Group 8 complexes $[(\text{tetraphos})\text{MH}(\eta^2\text{-H}_2)]^+$ by Bianchini *et al.* have shown the Ru species to display the weakest $d_\pi(\text{M}) \rightarrow \sigma^*(\eta^2\text{-H}_2)$ back-donation.²⁶

Hence, our NMR studies agree with those of other workers, in that the Fe complex **2** contains a more elongated dihydrogen ligand than its Ru analogue **4**. The implicitly stronger $\text{M}-(\eta^2\text{-H}_2)$ interaction in the first-row dihydrogen complex may possibly arise from an attractive ‘*cis*-effect’ between the hydride and the neighbouring dihydrogen ligand.²⁷ In the present case the H-H distance may well also be influenced by interactions with the $\text{OC}(\text{CF}_3)_2^-$ anion since **2** is in equilibrium with **1a** (Scheme 1).

We carried out DFT calculations on $[(\text{triphos})\text{Fe}(\text{CO})(\eta^2\text{-H}_2)\text{H}]^+$ **2**, to corroborate the structural parameters of the dihydrogen moiety obtained from the T_1 NMR measurements. Initially, we employed the same approach as in our calculations on **1**, with the six C_6H_5 substituents bound to the three P atoms of the triphos ligand being replaced with H atoms (**2'**). This resulted in a calculated H-H distance of 0.85 Å, implying a normal dihydrogen ligand rather than the elongated ligand of 1.03 Å suggested by the T_1 NMR measurements. It appeared at this stage that the simplified triphos ligand, calculated at the B3LYP level of theory with a 6-31G(d,p) basis set, had produced an inaccurate result through significant changes to the electronic nature of the ligand, and hence to the Fe centre, even though we have used this approach successfully for a closely related system.⁵ Accordingly, we proceeded to a full structural optimisation of **2**. The calculated structures and selected structural parameters of **2** and **2'** are presented in Fig. 5 and as Fig. S2,† respectively. In the event, the simplification of the triphos ligand appears to have had a negligible effect on the overall equilibrium structure, with an

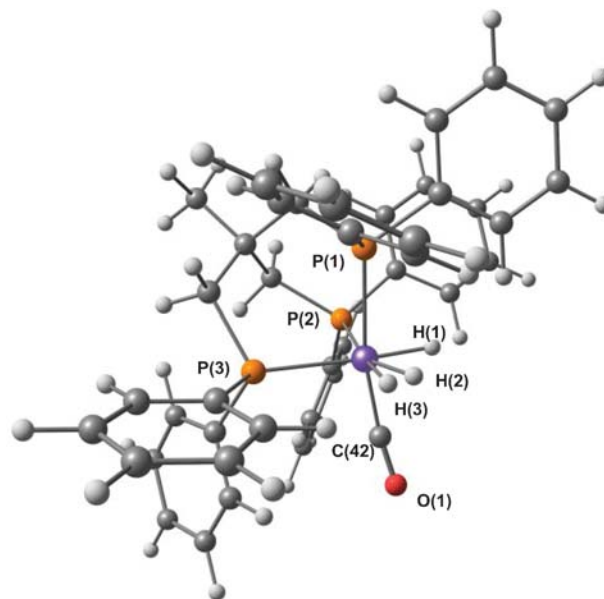


Fig. 5 DFT calculated structure of $[(\text{triphos})\text{Fe}(\text{CO})(\eta^2\text{-H}_2)\text{H}]^+$ (**2**) calculated at the B3LYP level of theory with a 6-31G(d,p) basis set. Selected bond lengths (in Å): Fe–H(1) 1.50, Fe–H(2) 1.57, Fe–H(3) 1.61, H(1)–H(2) 1.71, H(2)–H(3) 0.85, Fe–P(1) 2.323, Fe–P(2) 2.284, Fe–P(3) 2.312. Selected angles (in °): H(1)–Fe–H(2) 67.7, H(1)–Fe–H(3) 98.5, H(2)–Fe–H(3) 30.8, C(42)–Fe–H(1) 83.0, C(42)–Fe–H(2) 86.5, C(42)–Fe–H(3) 89.5, Fe–C(42)–O(1) 172.7, P(3)–Fe–H(1) 175.7, P(2)–Fe–H(2) 150.1, P(2)–Fe–H(3) 174.8, P(1)–Fe–C(42) 169.6.

H-H distance of 0.85 Å being obtained for **2**, identical to that deduced for **2'**.

This case is apparently similar to that of $[\text{OsCl}_2(\text{H}_2)(\text{NH}=\text{CPh}_2)(\text{P}^i\text{Pr}_3)_2]$, which was originally reported by Barea *et al.*,²⁸ and analysed in detail by Heinekey and co-workers.²⁹ Analogous NMR experiments to those presented above yielded a value of 1.24 Å for the H-H distance, virtually identical to that we obtained for **2**. Optimisation of the complex at the B3LYP level of theory yielded an H-H distance of 1.294 Å, with only a single minimum. However, the potential energy curve for the H-H stretching motion (calculated at several levels of theory) showed that varying the H-H distance between 1.00 and 1.60 Å, requires less than 4 kJ mol⁻¹; in other words, the H-H separation in this complex is virtually independent of energy. In this regime, oxidative addition and reductive elimination of the H_2 ligand can occur with essentially no activation barrier. In a similar vein, the complex $[\text{Cp}^*\text{Ru}(\text{dppm})(\text{H}_2)]^+$ exhibits an H-H distance of 1.10 Å as determined by neutron diffraction, which agrees well with the value calculated from T_1 measurements and J_{HD} measurements in solution.³⁰ Optimisation of the complex at the B3LYP level of theory correctly reproduced the experimental geometry, with the exception of the H-H and Ru-H distances.³¹ The H-H distance converged at 0.888 Å (a normal dihydrogen complex). This anomaly persisted when calculations were performed with extended basis sets, and the experimental geometry clearly did not conform to the ground state geometry derived from the calculations. Analysis of the

potential energy surface for the RuH_2 moiety revealed that the H_2 ligand is highly delocalised in $[\text{Cp}^*\text{Ru}(\text{dppm})(\text{H}_2)]^+$: the potential energy surface is highly anharmonic and the H–H and Ru– H_2 stretching modes are inseparable; there is extensive coupling between both degrees of freedom. The flat, anharmonic potential for the vibrationally coupled RuH_2 moiety in this system thus permits significant thermal population of higher vibrational states with large amplitudes of motion, leading to an average H–H distance in solution that is significantly longer than that derived for the electronic ground state by DFT methods. We are led to conclude that similar effects are at play in the case of $[(\text{triphos})\text{Fe}(\text{CO})(\eta^2\text{-H}_2)\text{H}]^+$ **2**, although an investigation of the potential energy surface of the $\text{MH}(\eta^2\text{-H}_2)$ moiety in this system is beyond the scope of our study. It is worth noting here that the discrepancy we observe for **2** between the average H–H distance in solution and the corresponding distance in the ground state may also exist for some of the other dihydrogen complexes of Group 8 discussed above, challenging the experimental conclusion that the $\text{M}(\eta^2\text{-H}_2)$ bond strength is actually weaker for Ru than for Fe.^{25,26}

Proton transfer to **1** via an Fe–H···H–O intermediate

Formation of **2** from **1** occurs through proton transfer from HFIP to an Fe–H moiety of **1**, as described in Scheme 2. The details of the reaction coordinate corresponding to this type of process have been the subject of vigorous investigations for the last decade.³² Although formation of $(\eta^2\text{-H}_2)$ species occurs via $\text{M}\text{-H}\cdots\text{H}\text{-X}$ intermediates, there is a dearth of characterised examples of this kind, on account of the low temperatures necessary to observe the labile $\text{M}\text{-H}\cdots\text{H}\text{-X}$ intermediate spectroscopically. The subtle chemical and physical changes in this multi-step process make it very complicated to study, and it is far from fully understood.³³

T_1 measurements through NMR spectroscopy provide a unique method for determination of $\text{M}\text{-H}\cdots\text{H}\text{-X}$ distances in such cases, because complexes containing these weak and

ephemeral proton–hydride interactions exist mainly in solution. There exist two NMR criteria for identifying $\text{M}\text{-H}\cdots\text{H}\text{-X}$ bonding. The first is a rather modest shift to low frequency of the hydride signal, which is temperature- and concentration-dependent. The second is a decrease in the spin–lattice relaxation time ($T_{1\text{min}}$) of the coordinated hydride ligand relative to the free hydride. Generally, $T_{1\text{min}}$ decreases by a factor of 1.5 to 3. Unfortunately, we were unable to determine the Fe–H···H–O distance in **1a**, owing to a lack of reproducibility in the T_1 values we measured.

NMR spectroscopy can also be useful for extracting thermodynamic data relating to the formation of proton–hydride complexes. Few attempts to determine thermodynamic parameters of proton transfer from an alcohol to a hydride have been reported in the literature, presumably on account of the complexity of the process.³⁴ Proton–hydride bond enthalpies can be obtained from the temperature-dependence of the formation constants of the corresponding intermediate (van't Hoff method). We studied the proton-transfer leading to the formation of $[(\text{triphos})\text{Fe}(\text{CO})\text{H}(\eta^2\text{-H}_2)]^+$ **2**, with the results shown in Fig. 6a. In this experiment, a two-fold excess of HFIP was introduced into a CD_2Cl_2 solution of **1** at 190 K in a 5 mm NMR tube. This produced a low-frequency shift of the hydride resonance, from $\delta = -10.80$ ppm to $\delta = -10.57$ ppm at 250 K (lower curve). In the absence of the proton donor, the chemical shift of the hydride resonance in **1** is practically independent of temperature (upper curve). This shift ($\Delta\delta = -0.23$ ppm) is reproducible and larger than the limits of experimental error, and demonstrates clearly the existence of an Fe–H···HOCH(CF_3)₂ interaction. Hence, the resonance at $\delta = -10.80$ ppm can be assigned to a hydrogen-bonded adduct of the type shown as **1a**.

Fig. 6b shows the strikingly similar results obtained from an analogous study of the protonation of $[(\text{triphos})\text{Ru}(\text{CO})\text{H}_2]$ **3** by Bakmutov and co-workers,⁶ who calculated ΔH°_f and ΔS°_f for a proton–hydride intermediate species **3a**. However, no experimental error was quoted for this study, nor was any possible contribution considered from a 1:2 hydrogen-bonded

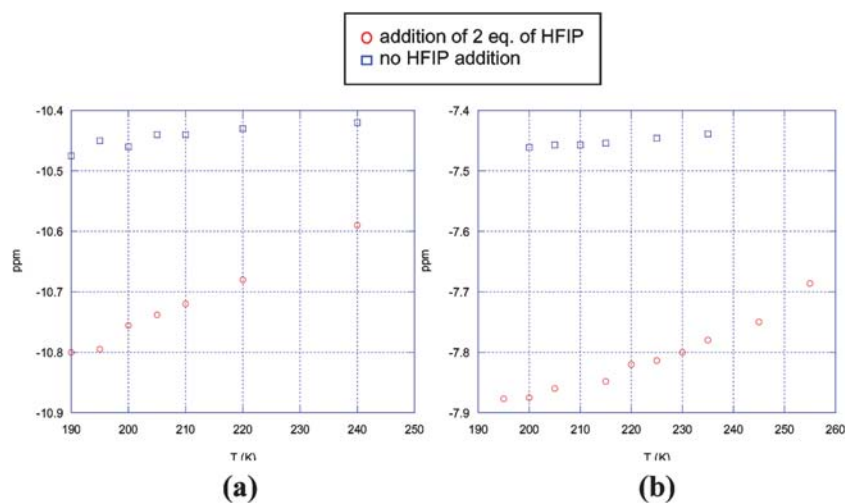


Fig. 6 (a) Temperature-dependence of the hydride chemical shift in CD_2Cl_2 solution of $[(\text{triphos})\text{Fe}(\text{CO})\text{H}_2]$ **1** (upper curve); and of **1** in the presence of a two-fold excess of HFIP (lower curve). (b) Temperature-dependence of the hydride chemical shift in CD_2Cl_2 solution of $[(\text{triphos})\text{Ru}(\text{CO})\text{H}_2]$ **3** (upper curve); and of **3** in the presence of a two-fold excess of HFIP (lower curve). Data for **3** are taken from ref. 6.

intermediate of the form [(triphos)M(CO)(H)H $\cdot\cdot$ HOCH(CF₃)₂], whose existence is impossible to discount in both the Fe and Ru systems, and whose involvement will vitiate any quantitative conclusions. Accordingly, we restrict our discussion to a qualitative comparison of the Fe and Ru intermediates **1a** and **3a**.

For [(triphos)Ru(CO)(H)H $\cdot\cdot$ HOCH(CF₃)₂] **3a**, ΔH°_f was calculated as $-29.7 \text{ kJ mol}^{-1}$, placing the adduct in the range of medium strength H-bonds, as expected.³² The chemical shift difference, $\Delta\delta$, between the free hydride complex [(triphos)M(CO)H₂] and the proton-hydride intermediate [(triphos)M(CO)(H)H $\cdot\cdot$ HOCH(CF₃)₂] is slightly greater for M = Ru (0.42 ppm) than for M = Fe (0.32 ppm); possibly implying a stronger M-H $\cdot\cdot$ H-X interaction in **3a** than in **1a**, and consistent with the higher basicity of **3** than of **1**.

The ΔS° value reported for formation of **3a** is $-79.5 \text{ J K}^{-1} \text{ mol}^{-1}$. In view of the higher fluxionality of the Fe system **1** as evidenced by its variable-temperature NMR spectra, we anticipate a larger loss of entropy in this system upon protonation to form the more rigid species **1a**. However, differences in M-H bond strengths, zero-point energy contributions, and the effects of solvation and electrostriction are impossible to assess; these can easily tip the balance in terms of entropy considerations.

Experimental

General

All operations were performed under an inert atmosphere with the use of Schlenk techniques and a glove box (MBraun, Labmaster 130), and using freshly distilled solvents. Routine ¹H and ³¹P NMR spectra were recorded using a Bruker AV360 spectrometer operating at 360 MHz, and 145 MHz, respectively, or a Bruker AV400 operating at 400 and 162. FT-IR spectra were recorded on a Perkin Elmer Spectrum One spectrometer with a beam-condensing accessory (BCA), using a diamond compression cell. Microanalyses were performed at the University of North London. *T*₁ measurements and VT NMR experiments were carried out in standard 5 mm NMR tubes in CD₂Cl₂ and the data were recorded using a Bruker DRX500 spectrometer operating at 500 or 202.5 MHz. If HFIP was added to the sample, this was carried out at -78°C by cooling the NMR tube in a dry ice-acetone bath, and the acid was transferred *via* a syringe. The mixture was degassed by passage of argon, and the Teflon valve was closed immediately. The NMR tube was then rapidly inserted into the probe of the spectrometer which had been pre-cooled to 190 K. All samples were allowed at least 10 min to equilibrate at each temperature. The conventional inversion-recovery method (180- τ -90) was used to determine the *T*₁ relaxation time as a function of temperature. Relaxation times were calculated using the non-linear three-parameter fitting routine of the spectrometers. The pulses were controlled at each temperature. In each experiment, the waiting period was much longer than the expected relaxation time, and 16 variable delays were employed. VT studies were performed in the range 190–300 K. Spectral simulations were carried out using gNMR (Cherwell Scientific Publishing Ltd, Oxford, version 4.1); the

rate constants derived from these simulations carry an estimated uncertainty of 10%.

Preparation of 1

[(triphos)FeH₂(CO)] was synthesised *via* two different methods.

Method A. A solution of NaBH₄ (0.3 g, 8 mmol) in ethanol (25 cm³) was added to a solution of [Fe(H₂O)₆][BF₄]₂ (0.337, 1 mmol) and triphos (0.625, 1 mmol) in THF (40 mL). The resulting solution was heated under reflux for 20 min to give a dark red solution. After filtration, a stream of CO (g) was passed through the solution for 10 min. The resulting dark orange solution was layered with hexane and stored at -40°C , producing a yellow powder after 1 d. The solution was reduced *in vacuo* to 20% and the remaining solution decanted. The precipitated solid was dried *in vacuo* and recrystallised from a mixture of CH₂Cl₂-EtOH. Yield: 23% (0.16 g, 0.23 mmol).

Method B. A vigorously stirred solution of [(triphos)-FeH(η^2 -BH₄)] (0.17, 0.24 mmol) in THF (7 mL) was treated with solid KO^tBu (0.08 g, 0.73 mmol), added in small portions. After 1 d stirring, the pink solution became orange-brown. This was filtered and a stream of CO (g) was passed through for 5 min. EtOH (6 mL) saturated with CO (g) was layered on top of the solution and left at -40°C to produce a yellow powder. Yield: 11% (0.08 g, 0.11 mmol). Anal. calc. for C₄₂H₄₁FeOP₃: C, 67.09; H, 5.49. Found: C, 68.34; H, 5.26%. IR (solid, cm⁻¹): ν_{CO} 1880 (br), ν_{FeH} 1663 (s). ¹H NMR (CD₂Cl₂, 295 K): δ 7.40–6.90 (m, 30H, phenyl H), 2.17 (s, 6H, CH₃(CH₂PPh₂)₃), 1.53 (s, 3H, CH₃(CH₂PPh₂)₃), -10.51 (q, 2H, FeH₂, ²*J*_{HP} = 21 Hz). ³¹P{¹H} NMR (CD₂Cl₂, 295 K): δ 57.12 (s). ¹H NMR (CD₂Cl₂, 200 K): δ 7.40–6.90 (m, 30H, phenyl H), 2.08 (m, 6H, CH₃(CH₂PPh₂)₃), 1.43 (s, 3H, CH₃(CH₂PPh₂)₃), -10.46 (2nd order, 2H, FeH₂, *T*_{change} = 260 K). ³¹P{¹H} NMR (CD₂Cl₂, 200 K): δ 61.31 (t, 1P, P_a, ²*J*_{P_aP_b} = 39.4), 54.9 (d, 2P, P_b). *T*_{1 min} = 208.06 ms (210 K).

Preparation of 2

A 5 mm NMR tube was charged in the glove-box with **1** (3.7 mg, 5.2 μmol) and CD₂Cl₂ (0.7 mL) was added. The NMR tube was cooled to -78°C , an excess of [(CF₃)₂CHOH] (10.4 μL , 8.3 μmol) was added *via* a syringe and the tube immediately sealed. The tube was rapidly inserted into the spectrometer probe maintained at 180 K, and the ¹H NMR spectrum immediately recorded at this temperature, revealing quantitative transformation of **1** into **2**. ¹H NMR (CD₂Cl₂, 200 K): δ 7.80–6.60 (m, 30H, phenyl H), 2.50–2.30 (br, 6H, CH₃(CH₂PPh₂)₃), 1.84 (br, 3H, CH₃(CH₂PPh₂)₃), -8.57 (br, 3H, FeH). ³¹P{¹H} NMR (CD₂Cl₂, 220 K): δ 45.96 (d, 2P, P_b, ²*J*_{P_aP_b} = 53.7 Hz), 41.25 (t, 1P, P_a). *T*_{1 min} = 20.61 ms (210 K).

Identification of the proton-hydride bonded adduct 1a

Under the experimental conditions described above, two equivalents of HFIP (1.3 μL , 1.0×10^{-2} mmol) were added *via* syringe to a solution of **1** prepared as described above. Low-temperature ¹H NMR spectra revealed the complete conversion of **1** into the proton-hydride bonded adduct **1a**. Addition of a subsequent 9.1 μL of HFIP resulted, as

described, in the formation of **2**. ^1H NMR (CD_2Cl_2 , 195 K): δ 7.80–6.60 (m, 30H, phenyl H), 2.50–2.30 (br, 6H, CH_3 - $(\text{CH}_2\text{PPh}_2)_3$), 1.82 (br, 3H, $\text{CH}_3(\text{CH}_2\text{PPh}_2)_3$), –10.80 (br, 3H, FeH). $^{31}\text{P}\{^1\text{H}\}$ NMR (CD_2Cl_2 , 220 K): δ 60.44 (t, 1P, P_a , $^2J_{\text{P}_a\text{P}_b} = 41.2$ Hz), 54.7 (d, 2P, P_b). T_1 measurements were not reproducible to the desired accuracy.

X-Ray crystallography studies

Suitable crystals of **1** were mounted on a thin glass fibre using silicon grease and cooled on the diffractometer to 120 K using Oxford Cryostream Liquid N_2 device. Approximate unit cell dimensions were determined by the Nonius Collect program using a Nonius $\text{K}\alpha$ CCD diffractometer (graphite monochromatic Mo- $\text{K}\alpha$ radiation, $\lambda = 0.71073$ Å), with a detector-to-crystal distance of 30 mm. Crystals were indexed using the DENZO-SMN package, and positional data were refined along with diffractometer constants to give the final unit cell parameters. Integration and scaling (DENZO-SMN, Scale-pack) resulted in unique data sets corrected for Lorentz and polarisation effects and for the effects of crystal decay and absorption, by a combination of averaging of equivalent reflections and an overall volume and scaling correction. Structures were solved using SHELXS-97 and developed *via* alternating least-squares cycles and difference Fourier synthesis (SHELXL-97). All non-hydrogen atoms were modelled anisotropically.

Crystal data for 1. $\text{C}_{42}\text{H}_{41}\text{FeOP}_3$, $M = 710.51$, yellow block, $0.30 \times 0.25 \times 0.25$ mm, monoclinic, space group $P2_1/n$ (No. 14), $a = 10.1997(3)$, $b = 18.1058(6)$, $c = 18.9884(7)$ Å, $\beta = 96.489(2)^\circ$, $V = 3484.2(2)$ Å³, $Z = 4$, $D_c = 1.354$ g cm⁻³, $F_{000} = 1488$, Nonius $\text{K}\alpha$ CCD, Mo- $\text{K}\alpha$ radiation, $\lambda = 0.71073$ Å, $T = 120(2)$ K, $2\theta_{\text{max}} = 50.0^\circ$, 17650 reflections collected, 5907 unique ($R_{\text{int}} = 0.1198$). Final GooF = 1.038, $R1 = 0.0588$, $wR2 = 0.0869$, R indices based on 3612 reflections with $I > 2\sigma(I)$ (refinement on F^2), 433 parameters, 0 restraints. Lp and absorption corrections applied, $\mu = 0.604$ mm⁻¹. The hydride atoms were located on the difference Fourier map, the thermal parameter of H(1) was fixed at 0.04, and both hydrides were refined freely.

DFT calculations on 1, 1', 2 and 2'

Gas phase structures and vibrational frequencies were calculated for each complex at the B3LYP level of theory with a 6-31G(d,p) basis set. Calculations were performed using Gaussian 03 on the Placentia2 cluster housed at the Memorial University of Newfoundland. Placentia2 is part of the ACEnet (Atlantic Computational Excellence Network) group of clusters in Maritime Canada.

Conclusions

The novel complex [(triphos)Fe(CO)H₂] **1** has been synthesised and characterised by ^1H and ^{31}P NMR and IR spectroscopies, and its structure has been determined by X-ray diffraction. Hence, it is shown to contain classical hydride ligands. Protonation of **1** by the medium strength acid HFIP gives the novel dihydrogen complex [(triphos)Fe(CO)H($\eta^2\text{-H}_2$)]⁺ **2**. Conventional NMR experiments and T_1 measurements have permitted

a thorough understanding of both **1** and **2**, and of the proton-transfer process which links them. The NMR experiments imply that complex **2** contains a stretched dihydrogen ligand ($r_{\text{HH}} = 1.23$ Å), with an H–H distance about 0.3 Å longer than in its Ru analogue **4**. This elongation apparently arises from a greater degree of $\text{M} \rightarrow (\eta^2\text{-H}_2)$ back-donation in **2** compared to in **4**, reversing the expected trend in H–H distances for dihydrogen complexes, which normally increases down a transition-metal triad. However, DFT calculations on **2** indicated a short H–H distance of 0.85 Å, characteristic of a normal dihydrogen ligand. A similar discrepancy between experimental and theoretical H–H distances has been noted for several other dihydrogen complexes of Group 8 metals. The proton-transfer process from HFIP to **1** proceeds through the proton-hydride hydrogen-bonded intermediate [(triphos)Fe(CO)(H)H \cdots HOCH(CF₃)₂] **1a**. A qualitative study of the M–H \cdots H–X bond in **1a** reveals a slightly lower basicity for the Fe complex **1** than for [(triphos)Ru(CO)H₂] **3**.

Acknowledgements

We thank King's College London for a studentship (to G.G.) and NSERC of Canada for financial support of this work. We also thank ACEnet for access to computational facilities.

References

- W. Hieber, *Ber. Dtsch. Chem. Ges.*, 1931, **64**, 2342.
- M. Torrent, M. Solà and G. Frenking, *Chem. Rev.*, 2000, **100**, 439 and references therein.
- M. A. Esteruelas and L. A. Oro, *Chem. Rev.*, 1998, **98**, 577.
- D. G. Gusev, R. Hubener, P. Burger, O. Orama and H. Berke, *J. Am. Chem. Soc.*, 1997, **119**, 3716 and references therein.
- G. Guilera, G. S. McGrady, J. W. Steed and N. Kaltsoyannis, *New J. Chem.*, 2004, **28**, 444.
- V. I. Bakhmutov, E. V. Bakhmutova, N. V. Belkova, C. Bianchini, L. M. Epstein, D. Masi, M. Peruzzini, E. S. Shubina, E. V. Vorontsov and F. Zanobini, *Can. J. Chem.*, 2001, **79**, 479.
- D. M. Heinekey and W. J. Oldham, Jr, *Chem. Rev.*, 1993, **93**, 913.
- See, for example, *Inorganic Chemistry. Principles of Structure and Reactivity*, ed. J. E. Huheey, E. A. Keiter and R. L. Keiter, Harper Collins, New York, 4th edn, 1993.
- F. Maseras, A. Lledós, E. Clot and O. Eisenstein, *Chem. Rev.*, 2000, **100**, 601.
- C. Soubra, Y. Oishi, T. A. Albright and H. Fujimoto, *Inorg. Chem.*, 2001, **40**, 620.
- C. Bianchini, F. Laschi, M. Peruzzini, F. M. Ottaviani, A. Vacca and P. Zanello, *Inorg. Chem.*, 1990, **29**, 3394.
- D. M. Heinekey and M. van Roon, *J. Am. Chem. Soc.*, 1996, **118**, 12134.
- M. T. Haward, M. W. George, P. Hamley and M. Poliakov, *J. Chem. Soc., Chem. Commun.*, 1991, 1101.
- E. S. Shubina, N. V. Belkova, A. N. Krylov, E. V. Vorontsov, L. M. Epstein, D. G. Gusev, M. Niedermann and H. Berke, *J. Am. Chem. Soc.*, 1996, **118**, 1105.
- P. A. Maltby, M. Schlaf, M. Steinbeck, A. J. Lough, R. H. Morris, W. T. Klooster, T. F. Koetzle and R. C. Srivastava, *J. Am. Chem. Soc.*, 1996, **118**, 5396.
- K. L. James, H. Mellows and D. M. Heinekey, *J. Am. Chem. Soc.*, 2001, **129**, 2085.
- X. L. Luo and R. H. Crabtree, *J. Am. Chem. Soc.*, 1990, **112**, 4813.
- N. Bampos and L. D. Field, *Inorg. Chem.*, 1990, **29**, 587.
- W. J. Oldham, Jr, A. S. Hinkle and D. M. Heinekey, *J. Am. Chem. Soc.*, 1997, **119**, 11028.
- (a) D. G. Hamilton and R. H. Crabtree, *J. Am. Chem. Soc.*, 1988, **110**, 4126; (b) P. J. Desrosiers, L. H. Cai, Z. R. Lin, R. Richards and J. Halpern, *J. Am. Chem. Soc.*, 1991, **113**, 4173.

- 21 M. T. Bautista, K. A. Earl, P. A. Maltby, R. H. Morris, C. T. Schweitzer and A. Sella, *J. Am. Chem. Soc.*, 1988, **110**, 7031.
- 22 R. H. Crabtree, *Angew. Chem., Int. Ed. Engl.*, 1993, **32**, 789.
- 23 See, for example, Ch. Elschenbroich and A. Salzer, *Organometallics*, VCH, Weinheim, 2nd edn, 1991.
- 24 C. Bianchini, M. Peruzzini and F. Zanobini, *J. Organomet. Chem.*, 1998, **354**, C19.
- 25 M. T. Bautista, E. P. Cappellani, S. D. Drouin, R. H. Morris, C. T. Schweitzer, A. Sella and J. Zubkowski, *J. Am. Chem. Soc.*, 1991, **113**, 4876 and references therein.
- 26 (a) C. Bianchini, K. Linn, D. Masi, M. Peruzzini, A. Polo, A. Vacca and F. Zanobini, *Inorg. Chem.*, 1993, **32**, 2366; (b) C. Bianchini, D. Masi, M. Peruzzini, M. Casarin, C. Maccato and G. A. Rizzi, *Inorg. Chem.*, 1997, **36**, 1061.
- 27 L. S. van der Sluys, J. Eckert, O. Eisenstein, J. H. Hall, J. C. Huffmann, S. A. Jackson, T. F. Koetzle, G. J. Kubas, P. J. Vergamini and K. G. Caulton, *J. Am. Chem. Soc.*, 1990, **112**, 4831.
- 28 G. Barea, M. A. Esteruelas, A. Lledos, A. M. Lopez and J. I. Tolosa, *Inorg. Chem.*, 1998, **37**, 5033.
- 29 D. M. Heinekey, A. Lledos and J. M. Lluch, *Chem. Soc. Rev.*, 2004, **33**, 175.
- 30 M. S. Cinn and D. M. Heinekey, *J. Am. Chem. Soc.*, 1987, **109**, 5865.
- 31 R. Gelabert, M. Moreno, J. M. Lluch and A. Lledos, *J. Am. Chem. Soc.*, 1997, **119**, 9840.
- 32 R. H. Crabtree, P. E. M. Siegbahn, O. Eisenstein, A. L. Rheingold and T. F. Koetzle, *Acc. Chem. Res.*, 1996, **29**, 348.
- 33 L. M. Epstein and E. S. Shubina, *Coord. Chem. Rev.*, 2002, **231**, 165.
- 34 J. A. Ayllon, C. Gervaux, S. Sabo-Etienne and B. Chaudret, *Organometallics*, 1997, **16**, 2000.